Enantioselectivity by Mass Spectrometry

by Maurizio Speranza

Understanding the detailed mechanism of transfer of chiral information between molecules in living systems and in supramolecular assemblies requires the quantification of the intrinsic short-range forces controlling enantioselectivity in simplified models, such as diastereomeric ion/molecule and molecule/molecule complexes in the isolated state. The most recent mass spectrometric achievements in this field are illustrated in the present review.

Chiral discrimination as observed in life chemistry is explained by the formation of weakly bound contact pairs between a chiral molecule (either the *R* or the *S* enantiomer) and a chiral selector *C*. Different noncovalent interactions operate in the diastereomeric complexes [*CR*] and [*CS*] [1] which, therefore, are endowed with a different stability (thermodynamic enantioselectivity, K_R vs K_S) and reactivity (kinetic enantioselectivity, k_R vs k_S) (Eq. 1).

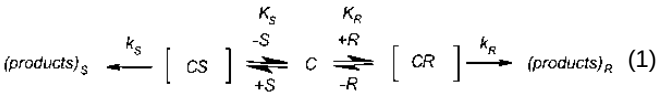

(1)

Quantification of noncovalent interactions in diastereomeric aggregates in the condensed phase represents a formidable task owing to the transient character of the adducts and the unavoidable interference from the medium [1].

To overcome these difficulties, increasing attention is being paid to gas-phase techniques, chiefly mass spectrometry (MS). Most intensive MS studies on gas-phase chiral discrimination have been carried out by using fast atom bombardment (FAB) or electrospray ionization (ESI) mass spectrometry, where the diastereomeric aggregates under investigation arise from desorption or vaporization of *C* and *R/S* dissolved in a liquid matrix. Despite the recognized versatility of these techniques, the ambiguity remains about the environment in which chiral discrimination occurs, whether in the bulk of the matrix, in its selvedge vaporization region, or in the gas phase. Furthermore, neither techniques ensure attainment of the equilibrium between $[CR]^+$ and $[CS]^+$ so that quantitative interpretation of their fragmentation patterns in terms of Eq. 1 is precluded. The latter restriction applies to the enantiodifferentiation of chiral molecules by chemical ionization mass spectrometry (CIMS) [3, 4]. For these reasons, the description of these MS methodologies to chiral discrimination [2] is beyond the specific purposes of this review and will not be considered further. The first part of this review is intended to focus exclusively on those MS procedures, such as FT-ICR or collision induced dissociation (CID) mass spectra, allowing quantification of enantioselectivity of chiral ionic aggregates by measuring their stability and reactivity (Eq. 1). The presentation is extended to neutral diastereomeric aggregates in the last part of the review.

M. Speranza, Dipartimento di Studi di Chimica e Tecnologia delle Sostanze Biologicamente Attive - Università di Roma "La Sapienza". maurizio.speranza@uniroma1.it

Enantioselectivity of Ionic Aggregates

The first quantitative FT-ICR study on asymmetric ion-molecule association involving chiral species was carried out by Nikolaev and coworkers [5], who determined the relative stability of the homochiral and the heterochiral dimers arising from self-protonation of a 1:1 mixture of the *L* and the *D* enantiomers of dimethyl- (**1**) and diisopropyl-tartrate (**2**).

$$Y = \frac{2\sqrt{([\mathbf{1}\cdot\mathrm{H}\cdot\mathbf{1}]^+[\mathbf{2}\cdot\mathrm{H}\cdot\mathbf{2}]^+}}{[\mathbf{1}\cdot\mathrm{H}\cdot\mathbf{2}]^+} \qquad (2)$$

The dimer chirality effect, expressed by the Y ratio of Eq. 2, is quantitatively evaluated at 20 °C and at different delay times (0.5-5 s) from the relative peak intensities of homogeneous (i.e. $[\mathbf{1}\cdot\mathrm{H}\cdot\mathbf{1}]^+$ and $[\mathbf{2}\cdot\mathrm{H}\cdot\mathbf{2}]^+$) and heterogeneous (i.e. $[\mathbf{1}\cdot\mathrm{H}\cdot\mathbf{2}]^+$) dimers. Despite these change appreciably with time, the Y ratio remains essentially constant at the values reported in Table 1. In the absence of chirality effects, the Y term must be the same for all four systems of Table 1. The ratio of the Y terms for the homochiral (Y_{homo}) and the heterochiral (Y_{hetero}) systems is equal to the equilibrium constant K_{eq} for the relevant ligand exchange reaction (e.g. $Y_{homo}/Y_{hetero}=K_{eq}$ for $[\mathbf{1}_L\cdot\mathrm{H}\cdot\mathbf{2}_L]^+ + \mathbf{2}_D \rightleftarrows [\mathbf{1}_L\cdot\mathrm{H}\cdot\mathbf{2}_D]^+ + \mathbf{2}_L$; Table 1).

Table 1 - Chiral discrimination of tartrates

Entry	*System*	*Y*	$K_{eq}=Y_{homo}/Y_{hetero}$	$\Delta G°_{298} = -RT\ln K_{eq}$ *(KJ mol^{-1})*
i	$\mathbf{1}_L + \mathbf{2}_L$	2.8	0.34	2.7
ii	$\mathbf{1}_L + \mathbf{2}_D$	8.3		
iii	$\mathbf{1}_D + \mathbf{2}_L$	8.4	0.32	2.8
iv	$\mathbf{1}_D + \mathbf{2}_D$	2.7		

The ESI-FT-ICR technique has been employed to measure at 350 K the equilibrium constants for the gas-phase $[\mathbf{3_S}\cdot H\cdot\mathbf{N_R}]^+ + \mathbf{4} \rightleftarrows [\mathbf{4}\cdot H\cdot\mathbf{N_R}]^+ + \mathbf{3_S}$ (K_R) and $[\mathbf{3_S}\cdot H\cdot\mathbf{N_S}]^+ + \mathbf{4} \rightleftarrows [\mathbf{4}\cdot H\cdot\mathbf{N_S}]^+ + \mathbf{3_S}$ (K_S) exchange reactions, where $\mathbf{N_R}$=(*R*)-α-(1-naphthyl)ethylamine and $\mathbf{N_S}$=(*S*)-α-(1-naphthyl)ethylamine (Scheme 1) [6]. The relevant K_R = 130±15 and K_S = 567±68 constants correspond to a $[\mathbf{3_S}\cdot H\cdot\mathbf{N_S}]^+$ vs. $[\mathbf{3_S}\cdot H\cdot\mathbf{N_R}]^+$ stability difference of 4.2±0.4 KJ mol^{-1} at 350 K. This stability difference is greater than that measured in methanol solution (2.3 KJ mol^{-1}), but similar to that seen in CD_2Cl_2 (4.6 KJ mol^{-1}) [7]. This points to the effects of solvation on the short-range intracomplex forces governing chiral discrimination.

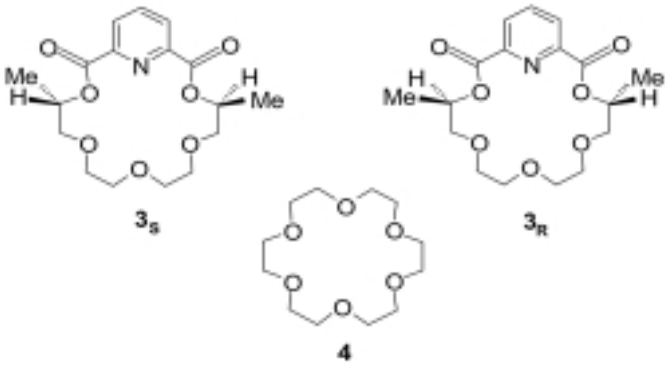

The same methodology was used to quantify the gas-phase $[\mathbf{3_R}\cdot H\cdot\mathbf{B_R}]^+ + \mathbf{B} \rightleftarrows [\mathbf{3_R}\cdot H\cdot\mathbf{B}]^+ + \mathbf{B_R}$ and $[\mathbf{3_S}\cdot H\cdot\mathbf{B_R}]^+ + \mathbf{B} \rightleftarrows \mathbf{3_S}\cdot H\cdot\mathbf{B}]^+ + \mathbf{B_R}$ equilibria, where $\mathbf{B_R}$ is the R enantiomer of *sec*-butylamine, α-cyclohexylethylamine, α-phenylethylamine, or α-(1-naphthyl)ethylamine, and **B** is an achiral amine, such as *iso*-propylamine or cyclohexylamine [8]. As observed in the previous study [6], binding of the guest with the absolute configuration opposite to that of the chiral crown ether is invariably preferred $(\Delta(\Delta G°) = \Delta G°([\mathbf{3_R}\cdot H\cdot\mathbf{B_R}]^+) - \Delta G°([\mathbf{3_S}\cdot H\cdot\mathbf{B_R}]^+) = 0.3\pm0.4$ ($\mathbf{B_R}$ = (*R*)-*sec*-butylamine), 0.9±0.2 ($\mathbf{B_R}$ = (*R*)-α-cyclohexylethylamine), 2.4±0.5 ($\mathbf{B_R}$ = (*R*)-α-phenylethylamine), and 3.5±0.6 ($\mathbf{B_R}$ = (*R*)-α-(1-naphthyl)ethylamine) KJ mol^{-1}.

A kinetic procedure has been employed to quantify the enantiodiscrimination of chiral amino acids by several protonated cyclodextrins [9, 10]. The inclusion complexes between the selected cyclodextrins and the amino acids are allowed to react with an achiral amine, e.g. 1-propylamine, into the FT-ICR analyzer cell. The exchange rates were measured and found to differ according to the nature and the configuration of the amino acid. Figure 1 reports the chiral selectivity (k_L/k_D) of the amino acids as a function of the number of carbons of their side chain (N). No correlation was found between the k_L/k_D ratios and the gas phase basicity of the amino acid. The linear correlation of Figure 1 is explained in terms of the cavity size effect on the inclusion complex. There exists an optimal size where chiral selectivity is favourable. For small amino acids with small side chains, such as Ala, even the cavity of the β-CD is too large. Both enantiomers of Ala can assume numerous types of coordination. Several of these would probably be similar, thereby decreasing selectivity. As the size of the side chain is increased (e.g. Ile and Leu), a complementary size is encountered that provides some limitations in the number of different complex structures but still allows the enantiomers to find favourable but distinct interactions. Strong steric interactions governs inclusion of aminoacids with a rigid side chain (Phe and Tyr) into the β-CD cavity so as to limit the number of different complex structures. For these amino acids, the cavity of the β-CD is too small to allow maximum chiral selectivity. Their selectivity is found to increse by increasing the cyclodextrin cavity, e.g. by using γ-CD instead of β-CD. Enantiodiscrimination of (*R*)- and (*S*)-2-butylamine was allowed by a ESI-FT-ICR kinetic study of their protonation by multiply charged [cytochrome *c*]$^{+n}$ (n=7-9) [11]. Proton transfer to the (*R*)-enantiomer is invariably faster than to (*S*)-one, irrespective of the charge state of cytochrome *c*.

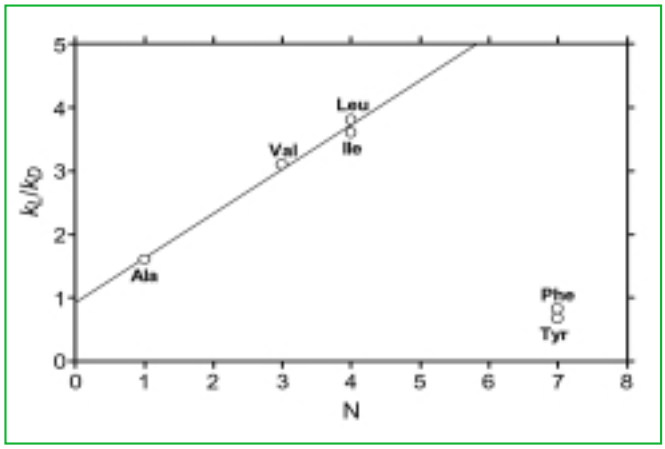

Figure 1 - Chiral selectivity as a function of the number of carbons (N) on the side chain of amino acids

Similarly, a FT-ICR study provided a means for discriminating (*R*)- and (*S*)-*sec*-butylacetates through the different ractivity of their protonated forms towards (*S,S,S*)-tri-*sec*-butylborate[12]. The relative stability of diastereomeric complexes, $[\mathbf{5_S}\cdot H^+\cdot\mathbf{6_S}]^-$ vs. $[\mathbf{5_R}\cdot H^+\cdot\mathbf{6_S}]^-$ and $[\mathbf{7_S}\cdot H^+\cdot\mathbf{8_R}]$ vs. $[\mathbf{7_R}\cdot H^+\cdot\mathbf{8_R}]$ (Scheme 2), was evaluated by using the kinetic method (T_{eff} = 333 K) [13, 14].

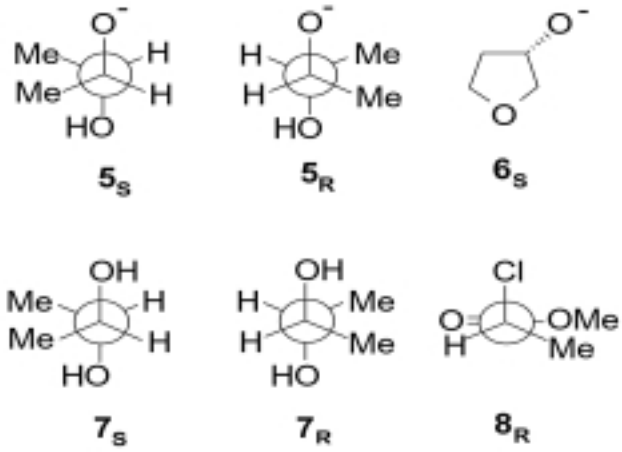

The relative abundances of their CID fragments ($[\mathbf{5_S}]/[\mathbf{6_S}]$ = 25.6; $[\mathbf{5_R}]/[\mathbf{6_S}]$ = 12.4; $([\mathbf{7_S}\cdot H^+]/[\mathbf{8_R}\cdot H^+]$ = 26.7; $([\mathbf{7_R}\cdot H^+]/[\mathbf{8_R}\cdot H^+]$ = 19.0) provide an estimate of the stability of their diastereomeric precursors $(\Delta(\Delta G°) = \Delta G°([\mathbf{5_R}\cdot H^+\cdot\mathbf{6_S}]^-) - \Delta G°([\mathbf{5_S}\cdot H^+\cdot\mathbf{6_S}]^-) = -1.67 + 2.14 = 0.47$ kcal mol^{-1}; $(\Delta(\Delta G°) = \Delta G°([\mathbf{7_R}\cdot H^+\cdot\mathbf{8_R}]) - \Delta G°([\mathbf{7_S}\cdot H^+\cdot\mathbf{8_R}]) = -1.94 + 2.17 = 0.23$ kcal mol^{-1}.

By the same token, chiral amino acids (**aa**) have been enantiodifferentiated in the gas phase based on the kinetics of the CID competitive fragmentation of their Cu(II)-bound trimers [15]. ESI of **aa**/$CuCl_2$ solutions into an ion trap MS reveals the presence of singly charged, covalently bound cluster ions of type $[Cu^{II}(\mathbf{aa})(\mathbf{ref})_2\text{-}H]^+$, where **ref** = chiral reference ligand, selected among the natural α-amino acids. These clusters under-

go CID competitive dissociation to form the dimeric complexes $[Cu^{II}(\mathbf{aa})(\mathbf{ref})\text{-}H]^+$and $[Cu^{II}(\mathbf{ref})_2\text{-}H]^+$, in proportions which depend on the configuration of **aa**. The CID results are given in Table 2. The chiral selectivity factor, R_{chiral} in Table 2, is expressed by the $[Cu^{II}(\mathbf{aa})(\mathbf{ref})\text{-}H]^+/[Cu^{II}(\mathbf{ref})_2\text{-}H]^+$ ratio for the *D*-enantiomer of **aa** relative to the same ratio for the *L*-enantiomer. The energy quantity $\Delta(\Delta Cu^{II}BDE)$ of Table 2 reflects the relative stability of the diastereomeric $[Cu^{II}(\mathbf{aa})(\mathbf{ref})\text{-}H]^+$ complexes. Their values indicate that **aa** with aromatic substituents display the largest chiral distinction, which is consistent with ligand exchange chromatographic results for analogous systems. It is concluded that the interactions between ligands, which determine chiral discrimination, are similar in solution and in the gas phase. The same procedure has been employed to enantiodiscriminate α-hydroxy acids [16]. A similar approach has been applied to the enantiodifferentiation chiral amino acids [17, 18] and aminophoshonic acids [19] by CID of their trimeric complexes $[M^I(\mathbf{aa})_2(\mathbf{ref})]^+$, with M^I=H, Li, Na, and K.

Table 2 - CID Fragmentation of $[Cu^{II}(aa)(ref)_2\text{-}H]+$ complexes (aa=amino acids)

Entry	***aa***	***ref***	*$[Cu^{II}(\mathbf{aa})(\mathbf{ref})\text{-}H]^+/[Cu^{II}(\mathbf{ref})_2\text{-}H]^+$*		*R_{chiral}*	*$\Delta(\Delta Cu^{II}BDE)$*
			D-enantiomer	*L-enantiomer*		*(kJ mol^{-1})*
i	Ala	L-Phe	0.049	0.024	2.0	2.1
ii	Val	L-Phe	0.75	0.17	4.5	4.3
iii	Leu	L-Phe	0.96	0.41	2.3	2.5
iv	Ile	L-Phe	1.7	0.36	4.8	4.6
v	Pro	L-Phe	12	2.2	5.3	4.9
vi	Asp	L-Phe	3.0	1.1	2.7	2.9
vii	Glu	L-Phe	11	3.7	3.1	3.3
viii	Ser	L-Phe	0.28	0.18	1.5	1.2
ix	Thr	L-Phe	1.4	0.76	1.8	1.7
x	Met	L-Trp	1.8	0.23	7.6	5.9
xi	Phe	L-Trp	0.11	0.013	8.3	6.2
xii	Tyr	L-Trp	0.21	0.019	11	6.9
xiii	Asn	L-Trp	6.1	3.3	1.8	1.7
xiv	Gln	L-Trp	50	7.3	6.8	5.6
xv	Trp	L-Asn	6.1	3.3	1.8	1.7
xvi	His	L-Arg	0.022	0.046	0.47	-2.2
xvii	Lys	L-His	0.91	1.6	0.56	-1.7

Enantioselectivity of molecular aggregates

The technique of supersonic expansion combined with electronic spectroscopy [20] has been recently applied to prepare and differentiate diastereomeric weakly bonded complexes [*CR*] and [*CS*] and to study under isolated conditions the nature of the forces responsible for chiral recognition [21-32]. Detailed structural characterization of the molecular complexes [*CR*] and [*CS*] is obtained using the resonance enhanced multiphoton ionisation (REMPI) spectroscopy, coupled with time-of-flight mass spectrometry (TOF) [25-32]. The supersonically expanded species under investigation, either the bare chromophore C or its molecular complexes [*CR*] and [*CS*], is ionized through absorption of several laser photons of adequate energy and mass selected by TOF. The species of interest is ionized through an R2PI process, i.e. one photon ν_1 is used to excite the species from its ground state S_0 to its first electronically excited state S_1 and a second photon, from the same laser beam (one-color R2PI or 1cR2PI; Figure 2a) or from another tuned at a different frequency ν_2 (two-color R2PI or 2cR2PI; Figure 2b), leads it to the continuum. The ν_1 wavenumber dependence of a given mass resolved ion represents the absorption spectrum of the species and contains important information about its electronic excited state S_1. In the 1cR2PI experiments on supersonically expanded clusters, some excess energy may be imparted to high-order complexes present in the beam which may partially decompose yielding the same ionic fragments arising from the 1:1 adduct (Figure 2a). These spurious signals usually complicate the interpretation of the spectrum of the 1:1 complex. This drawback is absent in the 2cR2PI experiments (Figure 2b) since, in this case, no significant excess energy is imparted to the complexes and decomposition of conceivable high-order clusters is strongly depressed. The mass resolved 1cR2PI spectrum of the bare chiral chromophore *C* may show several intense signals in the electronic $S_1 \leftarrow S_0$ band origin region. For instance, (*R*)-(+)-1-phenyl-1-propanol displays three bands at 37,577 (A), 37,618 (B), and 37,624 cm^{-1} (C) corresponding to three stable conformers [25-31], while the single adsorption at 37,618 cm^{-1}, exhibited by (*R*)-(+)-1-phenylethanol, demonstrates the presence of a single structure [32-33]. The R2PI absorption spectra of their molecular complexes normally show adsorption patterns which somewhat reproduce that of the bare chromophore but shifted toward the red or the blue. For instance, when *C*=(*R*)-(+)-1-phenyl-1-propanol, two most intense signals are observed, peak α of Figure 3, red-shifted relative to (A) by the $\Delta\nu_\alpha$ extent, and peak β of Figure 3, red-shifted relative to (B) by the $\Delta\nu_\beta$ quantity. The $\Delta\nu_\alpha$ and $\Delta\nu_\beta$ values of molecular complexes between *C* and a variety of achiral and chiral molecules (**solv**) are given in Figure 4 as a function of the proton affinity (PA) of **solv** [31].

A linear correlation is observed between the proton affinity of primary alcohols and the $\Delta\nu_\alpha$ and $\Delta\nu_\beta$ shifts of their complexes with (*R*)-(+)-1-phenyl-1-propanol. This observation allows to assign the α and β spectral signatures of Figure 3 to two different sets of molecular complexes, where the chromophore *C* is in a given conformation and acts as the hydrogen-bond donor to **solv** and where the alkyl group of **solv** maintains a specific spatial orientation toward the aromatic ring of *C*. In this case, both the electrostatic and the dispersive (polarization, charge exchange, etc.) interactions cooperate in stabilizing the adducts in the ground and excited states. The Δν values, mea-

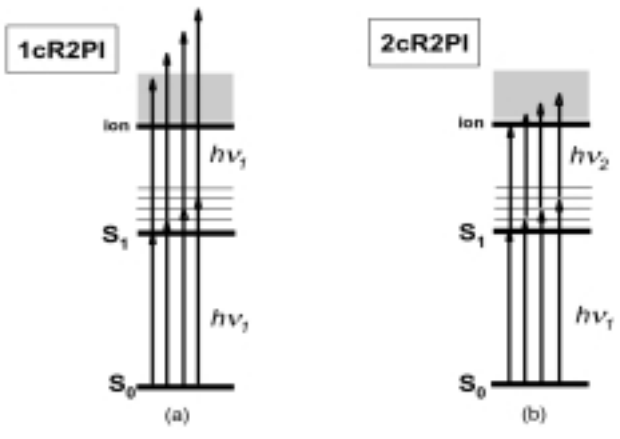

Figure 2 - Schematic representation of the 1cR2PI (a) and 2cR2PI experiments (b)

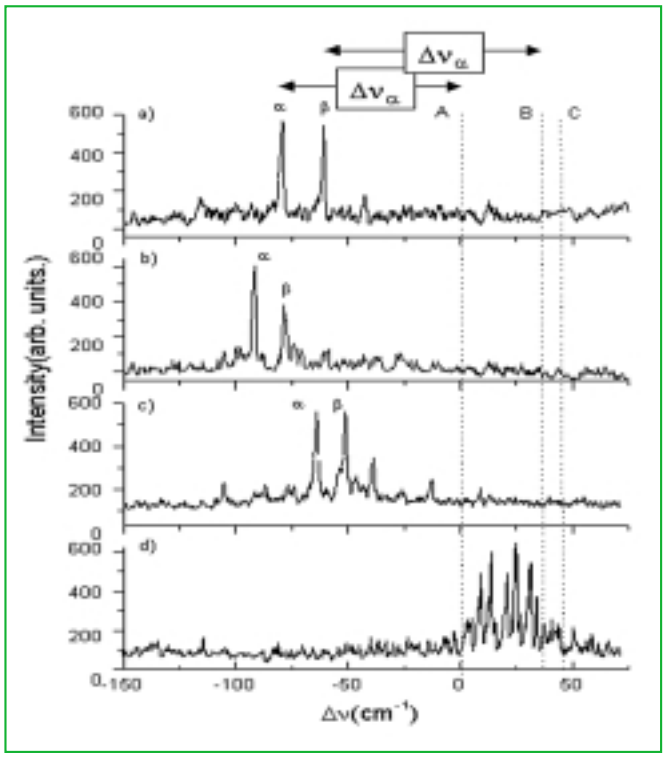

Figure 3 - 2cR2PI excitation spectra of the complexes between (R)-(+)-1-phenyl-1-propanol and solv = (R)-2-butanol (a), (S)-2-butanol (b), (R)-2-pentanol (c), and (S)-2-pentanol (d), measured at their m/z values and at a total stagnation pressure of 4x10^5 Pa

sured when **solv** = secondary alcohols and amines, are instead less negative than expected on the grounds of the linear correlation obtained for the primary alcohols. These deviations suggest that the relative contributions of electrostatic and dispersive forces in these systems are substantially different from those operating in the corresponding complexes with primary alcohols. Comparison of the $\Delta\nu$ values of diastereomeric complexes [*CR*] and [*CS*] with 2-butanols (**7**$_\alpha$ and **8**$_\alpha$ in Figure 4), 2-pentanols (**9**$_\alpha$ and **10**$_\alpha$ in Figure 4), and 2-butylamines (**12**$_\alpha$and **13**$_\alpha$ in Figure 4) indicates that the relative extent of electrostatic and dispersive forces depends upon the nature, the bulkiness, and the configuration of **solv**. In general, the homochiral complex [*CR*] exhibits a larger red shift than the heterochiral one [*CS*]. This implies an greater increase of the dispersive forces in the $S_1 \leftarrow S_0$ transition of [*CR*], relative to that occurring in [*CS*]. However, while the homochiral complex [*CR*] with *R*=(*R*)-2-pentanol exhibits a red shift ($\Delta\nu_\alpha$=-64 cm^{-1}), the corresponding heterochiral complex [*CS*] (*S*=(*S*)-2-pentanol) displays a blue shift difference ($\Delta\nu_\alpha$=+25 cm^{-1}) which strickingly contrasts with the larger red shifts observed in other heterochiral systems. This marked spectral diversity can be attributed to the greater steric congestion in [*CS*] (*S*=(*S*)-2-pentanol) which favors intense O-H$\cdots\pi$ electrostatic interaction (or even a change in the nature of the hydrogen-bond donor). Indeed, a similar blue shift is observed in the 1cR2PI absorption spectrum of the 1:1 cluster between *C* and water, where the solvent can establish with the aromatic ring of the chromophore only electrostatic O-H$\cdots\pi$ interactions [32-33]. Further insights into the forces operating in the molecular complexes between C and *solv* is obtained from the measurement of their binding energies [30-31]. The used procedure is summarized in Figure 5.

The binding energy D_0" of a molecular complexes is derived from the difference between its dissociative ionization threshold ($h\nu_1$'+$h\nu_3$') and the ionization threshold of bare C ($h\nu_1$+$h\nu_2$) (Figure 5a). The binding energy D_0' of the molecular complexes in the S_1 excited state is taken as equal to D_0"- $\Delta\nu$, using the appropriate $\Delta\nu$ terms of Figure 4. The dissociation energy D_0^+ of ionic cluster is obtained from the difference between its dissociative ionization threshold ($h\nu_1$'+$h\nu_3$') and its ionization threshold ($h\nu_1$'+$h\nu_2$') (Figure 5b). The 2cR2PI ionization thresholds correspond to the signal onset of the relevant ionic fragment obtained by scanning photon ν_2 while

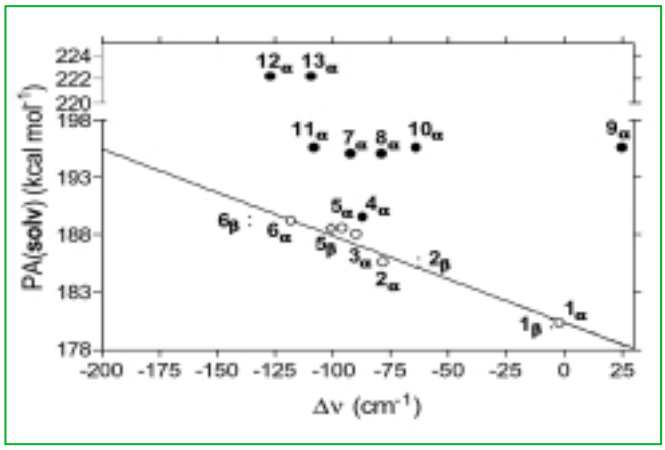

Figure 4 - Diagram of band origin shifts $\Delta\nu$ of the molecular complexes of (R)-(+)-1-phenyl-1-propanol with alcohols and amines. Open circles and diamonds refer respectively to the $\Delta\nu_\alpha$ and $\Delta\nu_\beta$ of the adducts with primary alcohols (methanol (1); ethanol (2); 1-propanol (3); 1-butanol (5); 1-pentanol (6)). Full circles refer to the $\Delta\nu_\alpha$ of the adducts with secondary alcohols (2-propanol (4); (S)-(+)-2-butanol (7); (R)-(-)-2-butanol (8); (S)-(+)-2-pentanol (9); (R)-(-)-2-pentanol (10); 3-pentanol (11)) and amines ((S)-(+)-2-butylamine (12); (R)-(-)-2-butylamine (13))

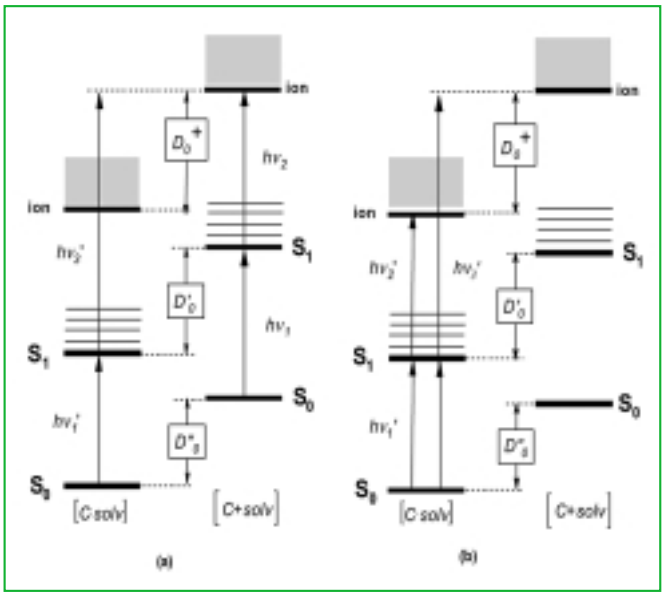

Figure 5 - Schematic representation of the energy levels of the bare C ([C +solv]) and of its complexes with solv ([C ·solv]). D"$_0$, D'$_0$, and D$^+_0$ as the binding energies of the adducts in the ground, excited,and ionized state, respectively

Table 3 - Phenomenological binding energies of molecular complexes

Entry	*C*[a]	***solv***	D_0'' *(kcal mol^{-1})*	D_0' *(kcal mol^{-1})*	D_0^+ *(kcal mol^{-1})*
i	(*R*)-(+)-PP	water	4.8±0.2	4.6±0.2	5.4±0.2
ii	(*R*)-(+)-PP	2-propanol	3.7±0.2	3.9±0.2	
iii	(*R*)-(+)-PP	1-butanol	2.6±0.2	2.9±0.2	6.5±0.2
iv	(*R*)-(+)-PP	(*R*)-2-butanol	5.9±0.2	6.1±0.2	8.4±0.2
v	(*R*)-(+)-PP	(*S*)-2-butanol	4.8±0.2	5.1±0.2	6.8±0.2
vi	(*R*)-(+)-PP	(*R*)-2-pentanol	4.7±0.2	4.9±0.2	8.5±0.2
vii	(*R*)-(+)-PP	(*S*)-2-pentanol	3.1±0.2	3.1±0.2	4.6±0.2
viii	(*R*)-(+)-PE	water	4.5±0.2	4.3±0.2	
ix	(*R*)-(+)-PE	(*R*)-2-butanol	1.9±0.5	2.3±0.5	
x	(*R*)-(+)-PE	(*S*)-2-butanol	0.9±0.5	1.3±0.5	

a) (*R*)-(+)-PP=(*R*)-(+)-1-phenyl-1-propanol, (*R*)-(+)-PE=(*R*)-(+)-1-phenylethanol

keeping v_1 at the fixed value corresponding to the $S_1 \leftarrow S_0$ transition. The relevant results are listed in Table 3. Concerning the diastereomeric complexes with chiral **solv**, the homochiral adducts are invariably more stable than the heterochiral ones. This trend extends to the corresponding S_1 excited complexes as well. This observation confirms the view that the interaction forces in these complexes are affected by steric congestion to a different extent.

Inspection of Table 3 reveals that the D_0^+ values always exceed the corresponding D_0'' interaction energies. The slow rise of the ion current observed in the 2cR2PI spectra suggests significant geometry change of the complex in its excited and the ionic state and, therefore, the phenomenological values of Table 3 are probably not representative of the actual binding energies of the relevant complexes [33]. Nevertheless, they provide an additional phenomenological tool for chiral recognition in the isolated state. Indeed, the relatively high D_0^+ values of the homochiral adducts (Table 3) are mirrored by less extensive fragmentation observed in the corresponding 1cR2PI/TOF mass spectra [34].

Conclusions

The advantages connected with studying enantioselectivity in simple complexes in the gas phase instead of in complicated associations in solution come from the possibility to make precise statements upon the nature and the structure of the complexes and to determine with great accuracy their relative stability and reactivity in the lack of any perturbing environmental effects. An array of MS methodologies have been developed to model intrinsic noncovalent interactions governing chiral discrimination in ionic and neutral complexes. The relevant results demonstrate that chiral discrimination in ionic and molecular aggregates is mainly determined by short-range attractive and repulsive (steric) forces and that these forces are dramatically affected by solvation.

It is hoped that the simultaneous development of more sophisticated MS devices and novel inlet systems for nonvolatile, fragile chirals will soon open the way to a deeper comprehension of the basic principles of enantioselectivity in molecular aggregates and, hence, of the intimate mechanisms of chemical information transfer in living systems which constitute the basis of millions of years of natural evolution.

References

[1] H.J. Schneider, *Angew. Chem. Int. Ed. Engl.,* 1991, **30,** 1417.

[2] a) M. Sawada, Biological Mass Spectrometry: Present and Future, T. Matsuo *et al.* (Eds.), Wiley, 1994, Chapter 3.19, p. 639; b) M. Sawada, *Mass Spectrometry Rev.,* 1997, **16,** 73.

[3] a) H.M. Fales, G.J. Wright, *J. Am. Chem. Soc.,* 1977, **99,** 2339; b) F.J. Winkler *et al., Tetr. Lett.,* 1986, **27,** 335; c) F.J. Winkler *et al., J. Chromatog. A,* 1994, **666,** 549; d) F.J. Winkler *et al., J. Mass Spectrom.,* 1997, **32,** 1072.

[4] a) H. Suming *et al., Org. Mass Spectrom.,* 1986, **21,** 7; b) N.M. Sellier *et al., Rapid Commun. Mass Spectrometry,* 1994, **8,** 891.

[5] E.N. Nikolaev *et al., Int. J. Mass Spectrom. Ion Proc.,* 1988, **86,** 249. See also: a) E.N. Nikolaev, T.B. McMahon, Proc. of the 43rd Annual Conference on Mass Spectrometry and Allied Topics, Atlanta, Georgia, 1995, 973; b) E.N. Nikolaev, E.V. Denisov, Proc. of the 44th Annual Conference on Mass Spectrometry and Allied Topics, Portland, Oregon, 1996, 415.

[6] I.H. Chu *et al., J. Am. Chem. Soc.,* 1993, **115,** 4318.

[7] R.B. Davidson *et al., J. Org. Chem.,* 1984, **49,** 353.

[8] D.V. Dearden *et al., J. Am. Chem. Soc.,* 1997, **119,** 353.

[9] J. Ramirez, F. He, C. B. Lebrilla, *J. Am. Chem. Soc.,* 1998, **120,** 7387.

[10] J. Ramirez *et al., J. Am. Chem. Soc.,* 2000, **122,** 6884.

[11] E. Camara *et al., J. Am. Chem. Soc.,* 1996, **118,** 8751.

[12] A. Filippi, M. Speranza, *Int. J. Mass Spectrom.,* 2000, **199,** 211.

[13] W. Shen *et al., Rapid Commun. Mass Spectrom.,* 1997, **11,** 71.

[14] R.G. Cooks *et al., Mass Spectrom. Rev.,* 1994, **13,** 287.

[15] a) W.A. Tao *et al., Anal. Chem.,* 1999, **71,** 4427; b) W.A. Tao *et al., J. Am. Chem. Soc.,* 2000, **122,** 10598.

[16] W.A. Tao, R.G. Cooks, *Angew. Chem.,* 2000, 2023.

[17] a) K. Vékey, G. Czira, *Anal. Chem.,* 1997, **69,** 1700; b) K. Vékey, G. Czira, *Rapid Commun. Mass Spectrom.,* 1995, **9,** 783.

[18] T. Vaisar *et al., J. Mass Spectrom.,* 1996, **31,** 937.

[19] A. Paladini *et al., Chirality,* 2001, **13,** 707.

[20] a) B. Brutschy, *Chem. Rev.,* 1992, **92,** 1567; b) H.J. Neusser, H. Krause, *Chem. Rev.,* 1994, **94,** 1829.

[21] A.R. Al-Rabaa *et al., Chem. Phys. Letters,* 1995, **237,** 480.

[22] A.R. Al-Rabaa *et al., J. Phys. Chem.,* 1997, **101,** 3273.

[23] K. Le Barbu *et al., J. Phys. Chem.,* 1998, **102,** 128.

[24] F. Lahmani *et al., J. Phys. Chem. A,* 1999, **103,** 1991.

[25] S. Piccirillo *et al., Angew. Chem. Int. Ed. Engl.,* 1997, **36,** 1729.

[26] A. Giardini Guidoni, S. Piccirillo, *Israel J. Chem.,* 1997, **37,** 439.

[27] A. Giardini Guidoni *et al., Proc. Indian Acad. Sci. (Chem. Sci.),* 1998, **110,** 1.

[28] A. Latini *et al., Chirality,* 1999, **11,** 376.

[29] M. Satta *et al., Chem. Phys. Letters,* 2000, **316,** 94.

[30] a) A. Latini *et al., Angew. Chem. Int. Ed. Engl.,* 1999, **38,** 815; b) A. Giardini Guidoni *et al., Chirality,* 2001, **13,** 727.

[31] A. Latini, M. Satta, A. Giardini Guidoni, S. Piccirillo, M. Speranza, *Chem. Eur. J.*, 2000, **6**, 1042.

[32] A. Giardini Guidoni *et al., Phys. Chem. Chem. Phys.,* 2000, **2,** 4139.

[33] M. Mons *et al., Phys. Chem. Chem. Phys.,* 2000, **2,** 5065.

[34] A. Filippi *et al., Int. J. Mass Spectrom.,* 2001, **210/211,** 483.

Acknowledgement: This work was supported by the Italian Ministero della Istruzione e della Ricerca Scientifica (MIUR) e dal Consiglio Nazionale delle Ricerche (CNR).